**High Resolution Electron Backscatter Diffraction Mapping of Shock-Deformation in Apatite from the Chicxulub Impact Structure.** Morgan A. Cox[1,2], Timmons M. Erickson[1,3], Martin Schmieder[2], and David A. Kring[2], [1]Space Science and Technology Centre (SSTC), School of Earth and Planetary Science, Curtin University, Perth, WA 6102, Australia. [2]Lunar and Planetary Institute (LPI) – USRA, 3600 Bay Area Boulevard, Houston, TX 77058, USA [3]Jacobs- JETS, Astromaterials Research and Exploration Science Division, NASA Johnson Space Center, Houston, Texas, 77058, USA. **(**Email: morgan.cox@student.curtin.edu.au)

**Introduction:** The phosphate apatite, $Ca_5(PO_4)_3(F,Cl,OH)$, is a ubiquitous accessory mineral found in both terrestrial and extraterrestrial rocks. It is commonly used to study planetary volatile abundances and, because it is a U–Pb carrier, to determine the ages of geologic events (e.g., [1]). The utility of apatite may be affected by impact cratering processes that produce shock-deformation microstructures within the phase, including planar fractures, partial to whole-scale recrystallization, and low angle grain boundaries, which have been observed in both terrestrial and extraterrestrial samples [2-6]. To better ascertain that type of deformation, we conducted a detailed microstructural analysis of crystals in ~550 m of shocked granitoid rocks and impact melt rocks in a core from the peak ring of the Chicxulub impact structure.

**Chicxulub Impact Structure:** The Chicxulub impact structure, located on the Yucatán Peninsula of Mexico, is ~180 km in diameter and exhibits the only well-preserved peak ring on Earth (e.g., [7,8]). The peak ring of the structure is ~80 to 90 km in diameter and rises ~400 m above the structural crater floor (e.g., [9]). In 2016 the International Ocean Discovery Program (IODP) and International Continental Scientific Drilling Program (ICDP) recovered 829 m of core from the peak ring of the Chicxulub crater during Expedition 364 [8,11]. The borehole M0077A consists of ~112 m of post-impact carbonates, ~130 m of impact melt rocks and (reworked) suevite, 587 m of coarse grained granitoid lithologies as well as pre-impact volcanic dikes and impact melt and breccia dikes [9,11].

Previously indexed orientations of planar deformation features (PDFs) and planar fractures (PFs) in quartz constrain shock pressures between ~12 and 17 GPa throughout the basement portion of the core [12]. Shock-deformation features have also been described within titanite crystals [13], along with the occurrence of the high-pressure polymorph $TiO_2$–II [14]. Here we complement those studies of shock deformation with new observations of shock-deformation in apatite from the peak-ring granites and in impact melt rock that experienced higher shock pressures.

**Samples and Methods:** Seventeen samples from the core were selected representing the interval 745 to 1320 meters below sea floor. The granitoid rocks (samples 95-2-82-84, 96-3-7-8.5, 111-2-77-78.5, 125-3-0-3, 150-3-25.5-27, 155-1-12-14, 168-3-25-27, 210-2-36-37.5, 237-2-60-61.5, 273-1-58-59.5, 276-1-85-87, 285-2-3-5, 299-2-10-12.5, 303-2-71-72.5) consist of plagioclase, quartz, alkali feldspar, biotite, with minor muscovite, apatite, zircon, titanite, epidote, garnet, ilmenite, and magnetite. The impact melt rock and melt veins (89-3-13.5-15, 163-3-52.5-54, 206-3-54-56) are aphanitic and mainly composed of quartz, feldspar, and calcite along with clasts of bedrock.

A total of 560 apatite crystals were identified and imaged using optical microscopy at the LPI. Back-scattered electron imaging using a JEOL-5910 scanning electron microscope (SEM) was then conducted at the NASA Johnson Space Center (JSC) in order to characterize microstructures within select apatite crystals.

Microstructural analyses of a subset of 108 apatite crystals were made with an Oxford Symmetry electron backscatter diffraction (EBSD) detector on a JEOL 7600f field emission gun SEM at JSC. Acquisition parameters included a 20 kV accelerating voltage, 18 nA beam current, 20.5 mm working distance, and 70° sample tilt. Step sizes of EBSD maps were between 700 to 50 nm.

**Results:** Apatite crystals range in length from 30 to 900 µm and exhibit euhedral to subhedral basal and prism crystal structures. Optical imaging of apatite crystals revealed planar fractures (PFs), sub-planar fractures, cataclastic deformation, and granular textures. All samples contain crystals with PFs; a total of ~250 apatite crystals contain PFs. Up to three orientations of PFs were identified within a single apatite crystal. Offsets along planar fractures are also identified in heavily fractured crystals, with up to ~5 µm of apparent displacement. Sub-planar fractures are common within apatite. Cataclastic deformation is present in 60 crystals and with some crystals sheared along fractures.

Seven apatite crystals within impact melt rock and melt veins in samples 89-3-13.5-15, 163-3-52.5-54 and 206-3-54-56, contain granular microstructures. Crystals are ~10 to 100 µm in size and contain a mixture of rounded neoblastic microstructures and larger euhedral laths.

Electron backscatter diffraction of 108 apatite crystals from granitoid and impact melt rock indicate plastic deformation affected apatite throughout the core. Crystals containing planar fractures (PFs) exhibit a higher degree of apparent deformation. Planar

deformation bands (PDBs) are observed in 5 crystals, with PDBs systematically misorientated up to 20˚ from the host in preferred crystallographic orientations (Fig. 1). Cataclastically deformed crystals exhibit >40˚ of mis-orientation of rotated fragments, with surrounding quartz showing high degree of crystal-plastic deformation as well.

High-resolution EBSD mapping of partially re-crystallized grains from impact melt shows that host apatite crystals contain large dispersions in pole figures due to impact-induced deformation, while newly recrystallized domains show little to no dispersion on pole figures indicating that they are strain-free domains. Fully re-crystallized grains show differences in crystallinity, with one grain containing a newly re-crystallized rim of apatite, while the interior of the crystal does not map by EBSD. Apatite included in sheet silicates show very low levels of crystal-plastic deformation, with <5º of misorientation observed, while crystals in contact with zircon and/or quartz show up to 20º misorientation across the crystal, with a high degree of deformation at the contact between apatite and zircon or quartz.

**Discussion:** Apatite microstructures observed throughout the core show varying levels of shock deformation from planar fractures, crystal-plastic deformation to complete recrystallization. Crystal-plastic deformation observed within apatite from the Chicxulub impact structure is similar to that described in apatite from the Paasselkä impact structure (Finland) [5] as well as in phosphate from lunar samples [4]. Planar deformation bands observed within apatite from our samples, however, are the first described from an impact structure. Planar deformation bands observed in the apatite crystals in this study are similar to those observed in zircon and xenotime from the Vredefort Dome and Santa Fe impact structures [15,16].

Recrystallization of apatite has been described at only a few impact structures, including lath-like crystals and rounded neoblasts in recrystallized crystals from the Paasselkä, Finland [5], Lac La Moinerie, Quebec [17], and Nicholson Lake, Northwest Territories [3] impact structures.

Further work that will be presented at the meeting includes field emission gun (FEG) electron microprobe analysis of recrystallized and partially recrystallized apatite crystals in order to quantify any possible changes in the volatile / halogen composition due to recrystallization, as well as high-resolution (~5 nm) transmission Kikuchi diffraction analyses and transmission electron microscopy data on apatite crystals with crystal-plastic deformation, specifically targeting planar deformation bands.

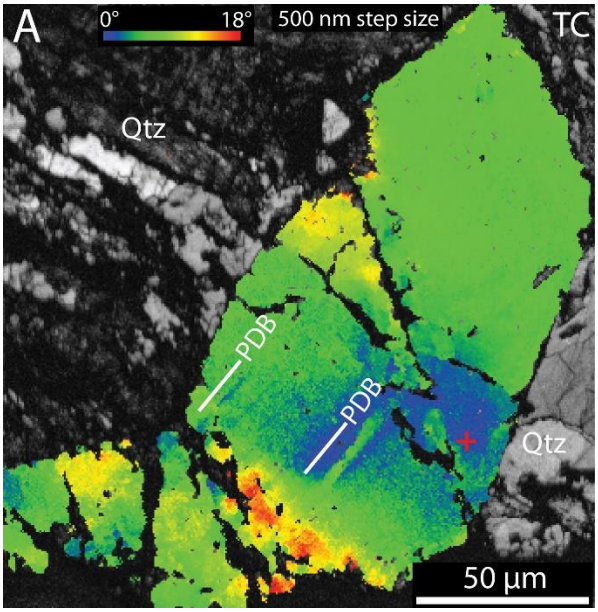


***Figure 1****. Texture component map showing mis-orientation within an apatite grain in shocked granitoid rock. The grain has PDBs that are up to 18º misoriented from the host grain. 168-3-25-27 (932.79 mbsf).*

**Acknowledgements:** Support was provided by the LPI Summer Intern Program in Planetary Sciences.

**References:** [1] Chew D. M. and Spikings R. A. (2015) *Elements 11*, 189–194. [2] Cavosie A. J. and Lugo Centeno C. (2014) *LPS XLV, Abstract #1691*. [3] McGregor M. et al. (2018) *Earth Planet. Sci. Lett., 504,* 185–197. [4] Černok A. et al. (2019) *Meteoritics & Planet. Sci,, 54*, 1262–1282. [5] Kenny G. et al. (2019) *LPS L*, Abstract #2132. [6] Shaulis B. J. et al. (2016) *LPS XLVII*, Abstract #2027. [7] Hildebrand A. R. et al. (1991) *Geology*, *19*,867–871. [8] Kring D. A. (2017) *GSA Today*, *27*, 4–8 [9] Gulick S. P S. et al. (2017) *Expedition 364 Preliminary Report: Chicxulub*. [10] Smit J. (1999) *Earth-Sci. Rev., 27*, 75–113. [11] Morgan J. V. et al. (2016) *Science*, *354*,878–882. [12] Rae A. et al. (2017) *LPS XLVIII*, Abstract #1934. [13] Timms N. E. et al. (2019) *Contrib. Min. Pet., 174*, 38–61. [14] Schmieder M. et al. (2019) *LPS L*, Abstract #2132. [15] Erickson T. M. et al. (2013) *Am. Mineral., 98*, 53–65. [16] Cavosie A. J. et al. (2016) *Geology*, *44*, 803–806. [17] McGregor M. et al. (2019) *Contrib. Min. Pet., 174*, 62–82.